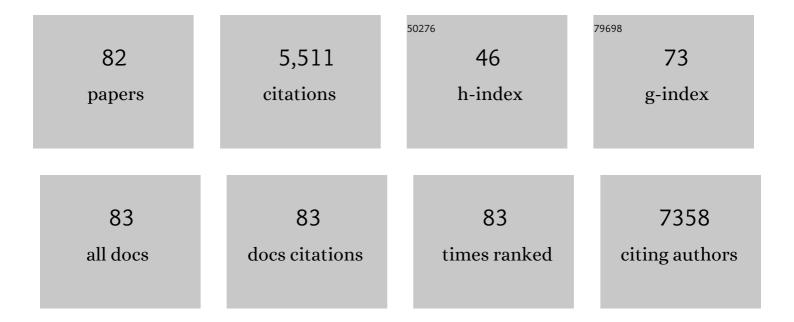
List of Publications by Year in descending order

Source: https://exaly.com/author-pdf/9464290/publications.pdf Version: 2024-02-01



#	Article	IF	CITATIONS
1	Hierarchical mesoporous NiCo2O4@MnO2 core–shell nanowire arrays on nickel foam for aqueous asymmetric supercapacitors. Journal of Materials Chemistry A, 2014, 2, 4795.	10.3	355
2	Chain-like NiCo2O4 nanowires with different exposed reactive planes for high-performance supercapacitors. Journal of Materials Chemistry A, 2013, 1, 8560.	10.3	250
3	Enhanced non-enzymatic glucose sensing based on copper nanoparticles decorated nitrogen-doped graphene. Biosensors and Bioelectronics, 2014, 54, 273-278.	10.1	215
4	ZnO nanorods on reduced graphene sheets with excellent field emission, gas sensor and photocatalytic properties. Journal of Materials Chemistry A, 2013, 1, 8445.	10.3	193
5	Design and synthesis of 3D interconnected mesoporous NiCo2O4@CoxNi1â^'x(OH)2 core–shell nanosheet arrays with large areal capacitance and high rate performance for supercapacitors. Journal of Materials Chemistry A, 2014, 2, 10090.	10.3	174
6	Colorimetric aptasensing of ochratoxin A using Au@Fe 3 O 4 nanoparticles as signal indicator and magnetic separator. Biosensors and Bioelectronics, 2016, 77, 1183-1191.	10.1	159
7	Visible light photoelectrochemical sensor for ultrasensitive determination of dopamine based on synergistic effect of graphene quantum dots and TiO 2 nanoparticles. Analytica Chimica Acta, 2015, 853, 258-264.	5.4	148
8	Mechanism analysis of the capacitance contributions and ultralong cycling-stability of the isomorphous MnO ₂ @MnO ₂ core/shell nanostructures for supercapacitors. Journal of Materials Chemistry A, 2015, 3, 6168-6176.	10.3	138
9	Label-free impedimetric aptasensor for detection of femtomole level acetamiprid using gold nanoparticles decorated multiwalled carbon nanotube-reduced graphene oxide nanoribbon composites. Biosensors and Bioelectronics, 2015, 70, 122-129.	10.1	127
10	Boosting the Visible-Light Photoactivity of BiOCl/BiVO ₄ /N-GQD Ternary Heterojunctions Based on Internal Z-Scheme Charge Transfer of N-GQDs: Simultaneous Band Gap Narrowing and Carrier Lifetime Prolonging. ACS Applied Materials & Interfaces, 2017, 9, 38832-38841.	8.0	119
11	Amplified impedimetric aptasensor based on gold nanoparticles covalently bound graphene sheet for the picomolar detection of ochratoxin A. Analytica Chimica Acta, 2014, 806, 128-135.	5.4	115
12	Multiple signal-amplification via Ag and TiO2 decorated 3D nitrogen doped graphene hydrogel for fabricating sensitive label-free photoelectrochemical thrombin aptasensor. Biosensors and Bioelectronics, 2018, 101, 14-20.	10.1	112
13	Magneto-controlled aptasensor for simultaneous electrochemical detection of dual mycotoxins in maize using metal sulfide quantum dots coated silica as labels. Biosensors and Bioelectronics, 2017, 89, 802-809.	10.1	108
14	AgBr nanoparticles/3D nitrogen-doped graphene hydrogel for fabricating all-solid-state luminol-electrochemiluminescence Escherichia coli aptasensors. Biosensors and Bioelectronics, 2017, 97, 377-383.	10.1	105
15	Nitrogen-Doped Graphene Quantum Dots@SiO ₂ Nanoparticles as Electrochemiluminescence and Fluorescence Signal Indicators for Magnetically Controlled Aptasensor with Dual Detection Channels. ACS Applied Materials & Interfaces, 2015, 7, 26865-26873.	8.0	104
16	MnO2 ultralong nanowires with better electrical conductivity and enhanced supercapacitor performances. Journal of Materials Chemistry, 2012, 22, 14864.	6.7	101
17	Self-assembling hybrid NiO/Co3O4 ultrathin and mesoporous nanosheets into flower-like architectures for pseudocapacitance. Journal of Materials Chemistry A, 2013, 1, 9107.	10.3	101
18	A sensitive Potentiometric resolved ratiometric Photoelectrochemical aptasensor for Escherichia coli detection fabricated with non-metallic nanomaterials. Biosensors and Bioelectronics, 2018, 106, 57-63.	10.1	97

#	Article	IF	CITATIONS
19	Engineering of Heterojunction-Mediated Biointerface for Photoelectrochemical Aptasensing: Case of Direct Z-Scheme CdTe-Bi ₂ S ₃ Heterojunction with Improved Visible-Light-Driven Photoelectrical Conversion Efficiency. ACS Applied Materials & Interfaces, 2017, 9, 18369-18376.	8.0	94
20	Magnetic-fluorescent-targeting multifunctional aptasensorfor highly sensitive and one-step rapid detection of ochratoxin A. Biosensors and Bioelectronics, 2015, 68, 783-790.	10.1	92
21	Perovskite-type BiFeO3/ultrathin graphite-like carbon nitride nanosheets p-n heterojunction: Boosted visible-light-driven photoelectrochemical activity for fabricating ampicillin aptasensor. Biosensors and Bioelectronics, 2019, 124-125, 33-39.	10.1	88
22	Facile one-pot synthesis of visible light-responsive BiPO4/nitrogen doped graphene hydrogel for fabricating label-free photoelectrochemical tetracycline aptasensor. Biosensors and Bioelectronics, 2018, 111, 131-137.	10.1	87
23	Label-free colorimetric aptasensor for sensitive detection of ochratoxin A utilizing hybridization chain reaction. Analytica Chimica Acta, 2015, 860, 83-88.	5.4	86
24	Design of a Dual Channel Self-Reference Photoelectrochemical Biosensor. Analytical Chemistry, 2017, 89, 10133-10136.	6.5	86
25	Hierarchical Nanorods of MoS ₂ /MoP Heterojunction for Efficient Electrocatalytic Hydrogen Evolution Reaction. Small, 2020, 16, e2002482.	10.0	85
26	Fabrication of magnetically assembled aptasensing device for label-free determination of aflatoxin B1 based on EIS. Biosensors and Bioelectronics, 2018, 108, 69-75.	10.1	83
27	One-pot synthesis of BiPO ₄ functionalized reduced graphene oxide with enhanced photoelectrochemical performance for selective and sensitive detection of chlorpyrifos. Journal of Materials Chemistry A, 2015, 3, 13671-13678.	10.3	78
28	A new strategy to effectively alleviate volume expansion and enhance the conductivity of hierarchical MnO@C nanocomposites for lithium ion batteries. Journal of Materials Chemistry A, 2017, 5, 21699-21708.	10.3	74
29	Magnetically controlled fluorescence aptasensor for simultaneous determination of ochratoxin A and aflatoxin B1. Analytica Chimica Acta, 2018, 1019, 119-127.	5.4	74
30	Recent developments of photoelectrochemical biosensors for food analysis. Journal of Materials Chemistry B, 2019, 7, 7283-7300.	5.8	72
31	Understanding the effect of polypyrrole and poly(3,4-ethylenedioxythiophene) on enhancing the supercapacitor performance of NiCo ₂ O ₄ electrodes. Journal of Materials Chemistry A, 2014, 2, 16731-16739.	10.3	70
32	Ultrasensitive electrochemical aptasensor for ochratoxin A based on two-level cascaded signal amplification strategy. Bioelectrochemistry, 2014, 96, 7-13.	4.6	65
33	An Interface Engineered Multicolor Photodetector Based on nâ€6i(111)/TiO ₂ Nanorod Array Heterojunction. Advanced Functional Materials, 2016, 26, 1400-1410.	14.9	64
34	MoS2/nitrogen doped graphene hydrogels p-n heterojunction: Efficient charge transfer property for highly sensitive and selective photoelectrochemical analysis of chloramphenicol. Biosensors and Bioelectronics, 2019, 126, 463-469.	10.1	64
35	Enhanced UV-visible light photodetectors with a TiO ₂ /Si heterojunction using band engineering. Journal of Materials Chemistry C, 2017, 5, 12848-12856.	5.5	61
36	Oxygen vacancy enhanced photoelectrochemical performance of Bi2MoO6/B, N co-doped graphene for fabricating lincomycin aptasensor. Biosensors and Bioelectronics, 2019, 135, 145-152.	10.1	60

#	Article	IF	CITATIONS
37	Design and synthesis of 3D hierarchical NiCo ₂ S ₄ @MnO ₂ core–shell nanosheet arrays for high-performance pseudocapacitors. RSC Advances, 2015, 5, 44642-44647.	3.6	57
38	Enhancing the Electrochemical Performance of Sodiumâ€lon Batteries by Building Optimized NiS ₂ /NiSe ₂ Heterostructures. Small, 2021, 17, e2104186.	10.0	56
39	Exceptional pseudocapacitive properties of hierarchical NiO ultrafine nanowires grown on mesoporous NiO nanosheets. Journal of Materials Chemistry A, 2014, 2, 12799-12804.	10.3	52
40	One-pot hydrothermal route to fabricate nitrogen doped graphene/Ag-TiO2: Efficient charge separation, and high-performance "on-off-on―switch system based photoelectrochemical biosensing. Biosensors and Bioelectronics, 2016, 83, 149-155.	10.1	51
41	Magnetically Separable Fe3O4 Nanoparticles-Decorated Reduced Graphene Oxide Nanocomposite for Catalytic Wet Hydrogen Peroxide Oxidation. Journal of Inorganic and Organometallic Polymers and Materials, 2013, 23, 907-916.	3.7	50
42	Amplified solid-state electrochemiluminescence detection of cholesterol in near-infrared range based on CdTe quantum dots decorated multiwalled carbon nanotubes@reduced graphene oxide nanoribbons. Biosensors and Bioelectronics, 2015, 73, 221-227.	10.1	49
43	Surface Coating Constraint Induced Anisotropic Swelling of Silicon in Si–Void@SiO <i>_x</i> Nanowire Anode for Lithiumâ€Ion Batteries. Small, 2017, 13, 1603754.	10.0	49
44	Nanoparticles Encapsulated in Porous Carbon Matrix Coated on Carbon Fibers: An Ultrastable Cathode for Liâ€ion Batteries. Advanced Energy Materials, 2017, 7, 1601363.	19.5	48
45	Hierarchical nanotubes constructed from CoSe2 nanorods with an oxygen-rich surface for an efficient oxygen evolution reaction. Journal of Materials Chemistry A, 2019, 7, 15073-15078.	10.3	47
46	CoMoO ₄ ·0.9H ₂ O nanorods grown on reduced graphene oxide as advanced electrochemical pseudocapacitor materials. RSC Advances, 2014, 4, 34307.	3.6	46
47	Fluorescent "on-off-on―switching sensor based on CdTe quantum dots coupled with multiwalled carbon nanotubes@graphene oxide nanoribbons for simultaneous monitoring of dual foreign DNAs in transgenic soybean. Biosensors and Bioelectronics, 2017, 92, 26-32.	10.1	46
48	Simultaneous detection of enrofloxacin and ciprofloxacin in milk using a bias potentials controlling-based photoelectrochemical aptasensor. Journal of Hazardous Materials, 2021, 416, 125988.	12.4	45
49	Carbon-coated mesoporous NiO nanoparticles as an electrode material for high performance electrochemical capacitors. New Journal of Chemistry, 2013, 37, 4031.	2.8	44
50	Preparation of graphene quantum dots based core-satellite hybrid spheres and their use as the ratiometric fluorescence probe for visual determination of mercury(II) ions. Analytica Chimica Acta, 2015, 888, 173-181.	5.4	44
51	Ingenious Dual-Photoelectrode Internal-Driven Self-Powered Sensing Platform for the Power Generation and Simultaneous Microcystin Monitoring Based on the Membrane/Mediator-Free Photofuel Cell. Analytical Chemistry, 2019, 91, 1728-1732.	6.5	42
52	One-pot synthesis of CdxZn1â^'xS–reduced graphene oxide nanocomposites with improved photoelectrochemical performance for selective determination of Cu2+. RSC Advances, 2013, 3, 14451.	3.6	38
53	Synchronized purification and immobilization of his-tagged β-glucosidase via Fe3O4/PMG core/shell magnetic nanoparticles. Scientific Reports, 2017, 7, 41741.	3.3	38
54	One-Step Low-Temperature Molten Salt Synthesis of Two-Dimensional Si@SiO <i>_x</i> @C Hybrids for High-Performance Lithium-Ion Batteries. ACS Applied Materials & Interfaces, 2020, 12, 55844-55855.	8.0	36

#	Article	IF	CITATIONS
55	Photoelectrochemical aptasensor for sensitive detection of tetracycline in soil based on CdTe-BiOBr heterojunction: Improved photoactivity enabled by Z-scheme electron transfer pathway. Journal of Hazardous Materials, 2022, 424, 127498.	12.4	36
56	Immobilization of cellulase on thermo-sensitive magnetic microspheres: improved stability and reproducibility. Bioprocess and Biosystems Engineering, 2018, 41, 1051-1060.	3.4	34
57	Facile Preparation of Unsubstituted Iron(II) Phthalocyanine/Carbon Nitride Nanocomposites: A Multipurpose Catalyst with Reciprocally Enhanced Photo/Electrocatalytic Activity. ACS Sustainable Chemistry and Engineering, 2019, 7, 3319-3328.	6.7	33
58	Reactable ionic liquid assisted preparation of porous Co3O4 nanostructures with enhanced supercapacitive performance. CrystEngComm, 2014, 16, 2395.	2.6	32
59	Photoelectrochemical CaMV35S biosensor for discriminating transgenic from non-transgenic soybean based on SiO2@CdTe quantum dots core-shell nanoparticles as signal indicators. Talanta, 2016, 161, 211-218.	5.5	32
60	Fabrication of l -cysteine-capped CdTe quantum dots based ratiometric fluorescence nanosensor for onsite visual determination of trace TNT explosive. Analytica Chimica Acta, 2016, 946, 80-87.	5.4	29
61	A novel universal colorimetric sensor for simultaneous dual target detection through DNA-directed self-assembly of graphene oxide and magnetic separation. Chemical Communications, 2017, 53, 7096-7099.	4.1	29
62	A homogeneous assay for highly sensitive detection of CaMV35S promoter in transgenic soybean by förster resonance energy transfer between nitrogen-doped graphene quantum dots and Ag nanoparticles. Analytica Chimica Acta, 2016, 948, 90-97.	5.4	28
63	Stabilizing Lithium–Sulfur Batteries through Control of Sulfur Aggregation and Polysulfide Dissolution. Small, 2018, 14, e1703816.	10.0	28
64	Horseradish peroxidase immobilized on the magnetic composite microspheres for high catalytic ability and operational stability. Enzyme and Microbial Technology, 2019, 122, 26-35.	3.2	28
65	Amplified photocurrent signal for fabricating photoelectrochemical sulfadimethoxine aptasensor based on carbon nitride photosensitization with visible/near-infrared light responsive zinc phthalocyanine. Journal of Hazardous Materials, 2021, 406, 124749.	12.4	28
66	In situ transmission electron microscopy study of individual nanostructures during lithiation and delithiation processes. Journal of Materials Chemistry A, 2017, 5, 20072-20094.	10.3	27
67	Reversible formation of networked porous Sb nanoparticles during cycling: Sb nanoparticles encapsulated in a nitrogen-doped carbon matrix with nanorod structures for high-performance Li-ion batteries. Journal of Materials Chemistry A, 2019, 7, 24292-24300.	10.3	23
68	Enhanced cathodic electrochemiluminescent microcystin-LR aptasensor based on surface plasmon resonance of Bi nanoparticles. Journal of Hazardous Materials, 2022, 434, 128877.	12.4	20
69	Visible light-driven photoelectrochemical ampicillin aptasensor based on an artificial Z-scheme constructed from Ru(bpy)32+-sensitized BiOI microspheres. Biosensors and Bioelectronics, 2021, 173, 112771.	10.1	19
70	Hydrothermal control growth of Zn2GeO4–diethylenetriamine 3D dumbbell-like nanobundles. CrystEngComm, 2014, 16, 3222.	2.6	17
71	"Signal on―electrochemiluminescence pentachlorophenol sensor based on luminol-MWCNTs@graphene oxide nanoribbons system. Talanta, 2015, 134, 448-452.	5.5	16
72	Red Phosphorus Anchored on Nitrogenâ€Doped Carbon Bubbleâ€Carbon Nanotube Network for Highly Stable and Fastâ€Charging Lithiumâ€Ion Batteries. Small, 2022, 18, e2105866.	10.0	16

#	Article	IF	CITATIONS
73	Molten Au/Ge Alloy Migration in Ge Nanowires. Nano Letters, 2015, 15, 2809-2816.	9.1	15
74	Enhanced electrochemiluminescence sensing platform using nitrogen-doped graphene as a novel two-dimensional mat of silver nanoparticles. Talanta, 2015, 132, 146-149.	5.5	15
75	Multifunctional NiCo ₂ O ₄ nanosheet-assembled hollow nanoflowers as a highly efficient sulfur host for lithium–sulfur batteries. Dalton Transactions, 2020, 49, 6876-6883.	3.3	13
76	Ethanol gas sensor based on a self-supporting hierarchical SnO ₂ nanorods array. CrystEngComm, 2015, 17, 1800-1804.	2.6	12
77	Copper(I) oxide nanospheres decorated with graphene quantum dots display improved electrocatalytic activity for enhanced luminol electrochemiluminescence. Mikrochimica Acta, 2016, 183, 1591-1599.	5.0	12
78	Enhanced conductivity and structure stability of BiPO ₄ @void@C/CNT particles for high-performance bismuth-based batteries. Dalton Transactions, 2020, 49, 5636-5645.	3.3	9
79	A facile approach for the synthesis of Cu2â^'x Se nanowires and their field emission properties. Journal of Materials Science, 2014, 49, 532-537.	3.7	6
80	Simultaneous detection of TNOS and P35S in transgenic soybean based on magnetic bicolor fluorescent probes. Talanta, 2020, 212, 120764.	5.5	6
81	Improving the cycling stability of lithium–sulfur batteries by hollow dual-shell coating. RSC Advances, 2018, 8, 9161-9167.	3.6	3
82	Co0.85Se particles encapsulated in the inner wall of nitrogen-doped carbon matrix nanotubes with rational interfacial bonds for high-performance lithium-ion batteries. Dalton Transactions, 2021, 50, 11458-11465.	3.3	3